



PERGAMON

Solid State Communications 123 (2002) 11–15

solid
state
communicationswww.elsevier.com/locate/ssc

Ultraviolet photoelectron spectroscopy study of colossal magnetoresistive $\text{La}_{0.7-x}\text{Pr}_x\text{Ca}_{0.3}\text{MnO}_3$

C.-W. Lee^a, Y.D. Zhao^a, H. Koh^a, H.-J. Noh^a, J. Park^a, H.-D. Kim^a, J. Yu^a, S.-J. Oh^{a,*},
M. Han^b

^aCenter for Strongly Correlated Materials Research and Department of Physics, Seoul National University, Seoul 151-742, South Korea

^bDepartment of Physics, University of Seoul, Seoul 130-743, South Korea

Received 28 March 2002; received in revised form 28 March 2002; accepted 8 May 2002 by E. Molinari

Abstract

We have investigated the electronic structure of colossal magnetoresistive perovskite manganites $\text{La}_{0.7-x}\text{Pr}_x\text{Ca}_{0.3}\text{MnO}_3$ using ultraviolet photoelectron spectroscopy as a function of temperature and Pr concentration x ($x = 0.13, 0.3, \text{ and } 0.4$). Unusual temperature-dependent and x -dependent spectral changes are observed in the entire valence band region. Since Pr doping does not introduce carriers into the system but brings about strong lattice distortion effects which exert significant influence on the p - d hybridization, the degree of mixing between Mn 3d and O2p levels is considered to be the major factor responsible for the spectral weight transfers with temperature and Pr doping level. The observed changes are not consistent with the results of local-density-approximation (LDA) band calculation, but can be understood by the density-of-states from the LDA + U calculation or configuration-interaction cluster calculations. This implies that a strong correlation effect between d electrons plays an important role in these manganites. High resolution spectra near the Fermi level shows a clear metallic edge at low temperature for low Pr concentration sample ($x = 0.13$), but the metallic Fermi edge disappears at higher Pr doping levels ($x = 0.3$ and 0.4) even at the temperature below T_c where the bulk metal–insulator transition occurs. This may be due to the low effective carrier density resulting from the reduced ferromagnetic ordering and the lattice distortion, or the pseudo-gap phenomena and the surface effect. © 2002 Elsevier Science Ltd. All rights reserved.

PACS: 79.60. - i; 71.20. - b; 71.27. + a; 71.30. + h

Keywords: A. Magnetically ordered materials; D. Electronic band structure; E. Photoelectron spectroscopies

One of the most active areas of current interest in the field of transition metal compounds is the physics of the perovskite manganites with the chemical formula $\text{R}_{1-x}\text{A}_x\text{MnO}_3$, (R is a rare earth metal such as La, Pr, Nd, Sm, Gd; A is a divalent element such as Ca, Sr, Ba). Main reason for the attention is the colossal magnetoresistance (CMR) effects observed in these compounds [1]. It is interesting that the CMR effects are found in the presence of the coexistence of metal–insulator transition and ferromagnetic ordering transition. The coexistence of ferromagnetic ordering and metallic behavior below the transition temperature T_c has been

traditionally explained within the framework of double exchange (DE) model [2–4]. Doped manganites are mixed-valent compounds containing both $\text{Mn}^{3+}(t_{2g}^3e_g^1)$ and $\text{Mn}^{4+}(t_{2g}^3)$ ions. According to the DE model, the e_g electrons are mobile charge carriers interacting with the Mn^{4+} ($S = 3/2$) background. The carrier hopping depends on the relative alignment of the carrier spin to the localized Mn^{4+} spin. When the two spins are aligned, the carrier hops easily since the on-site Hund exchange energy is substantially reduced. But the insulating behavior above T_c cannot be explained by this DE model alone. Thus it was proposed that some additional effects are needed to reduce the carrier hopping substantially. Millis et al. [5–7] proposed that a strong Jahn-Teller distortion and a ‘breathing’ distortion of electron–phonon coupling play an important role. Extended

* Corresponding author. Tel.: +82-2-880-6609; fax: +82-2-877-6796.

E-mail address: sjoh@phy.snu.ac.kr (S.J. Oh).

X-ray absorption fine structure (EXAFS) [8] and neutron pair distribution function [9] experiments have given evidence for the predicted existence of local lattice distortions. Spectroscopic studies have also been carried out to get the microscopic understanding of electronic structure of these manganites. J.-H. Park et al. [10] investigated the electronic structure of $\text{La}_{1-x}\text{Ca}_x\text{MnO}_3$ and $\text{La}_{1-x}\text{Pb}_x\text{MnO}_3$, and found that strong small polaron effects are responsible for the low conductivity above T_c . Temperature-dependent electronic structure was also studied for $\text{La}_{1-x}\text{Sr}_x\text{MnO}_3$ [11–13] and $\text{Pr}_{1-x}\text{Sr}_x\text{MnO}_3$ [14,15].

In this work, we report the ultraviolet photoemission spectroscopy (UPS) study of $\text{La}_{0.7-x}\text{Pr}_x\text{Ca}_{0.3}\text{MnO}_3$ (LPCMO) with $x = 0.13, 0.3, \text{ and } 0.4$. This system is interesting in that as the Pr content x is varied, many physical properties such as resistivity and magnetization change dramatically while the carrier concentration remains the same. Hwang et al. first made a systematic investigation on the transport and magnetic properties of $\text{La}_{0.7-x}\text{Pr}_x\text{Ca}_{0.3}\text{MnO}_3$ series for $x = 0–0.7$ [16], and found that dc resistivity at low temperature changes by several orders of magnitude with Pr concentration, while the magnetization continuously decreases as the Pr content increases from 0.175 to 0.7. They interpreted these results as due to the change of Mn–O–Mn bond angle with Pr content. In the AMnO_3 perovskite manganese oxide, Mn ions occupy the B site and are surrounded by oxygen octahedra which share corners, while La and Pr ions occupy the A site between these octahedra. The electronically active band is formed by the overlap between Mn d orbital and oxygen p orbitals. This overlap can be strongly influenced by the internal pressure generated by the A site substitution with ions of different radii. This effect is quantified by the tolerance factor $t = (\text{A–O})/[\sqrt{2}(\text{Mn–O})]$, which is a simple characterization of the size mismatch in the perovskite structure. For a perfect match $t = 1$, the A-site ions have just the right size to fill the space in three-dimensional network of MnO_6 octahedra and the Mn–O–Mn bond angle $\theta = 180^\circ$. When $t < 1$, the Mn–O bond is placed under compression and the A–O bond under tension. The MnO_6 octahedra will tilt and rotate to alleviate these stresses. These tilting and rotations bend θ from 180° to $(180^\circ - \phi)$, and ϕ increases as t decreases. In the case of LPCMO, t is reduced as Pr content x increases because the size of Pr ion is smaller than that of La ion, therefore leading to the decrease of θ . Since the p–d hybridization strength is proportional to $\sin(\theta/2)$ in the simple DE model, the hybridization is reduced when Pr doping level increases.

The temperature T also influences the transport property of LPCMO since the hopping of the e_g electron carrier depends greatly on the degree of ferromagnetic order in the DE model. As temperature goes down below T_c , the ferromagnetic order is enhanced, resulting in the increase of electron hopping. Hence we can say that the effective mixing between Mn 3d and oxygen 2p levels become

enhanced when the temperature is lowered below T_c and the Pr concentration is reduced. Indeed the optical conductivity of LPCMO samples found that the effective carrier density N_{eff} is strongly dependent on temperature T and Pr content x [17,18]. When $T > T_c$, N_{eff} is almost independent of T and x . But when $T < T_c$, N_{eff} increases rapidly as the temperature is lowered while it decreases remarkably when x increases from 0.13 to 0.4. In our present photoemission experiments on LPCMO, we observed an unusual redistribution of spectral weight in the whole valence band (VB) region as we changed temperature and Pr content. We also found the loss of clear metallic Fermi edge even at temperature below the bulk metal–insulator transition at higher Pr-doping levels. We interpret these results in terms of Mn 3d–O 2p hybridization effect on the density of states within the local-density-approximation (LDA) + U calculation.

Polycrystalline $\text{La}_{0.7-x}\text{Pr}_x\text{Ca}_{0.3}\text{MnO}_3$ samples with $x = 0.13, 0.3$ and 0.4 were synthesized by a standard solid state reaction method as described in detail in Refs. [17,18]. X-ray powder diffraction (XRD) showed all samples were single-phase. Electron probe microanalyses confirmed that the samples were stoichiometric [19,20]. Both resistivity and magnetization curves showed hysteretic behavior, indicating that corresponding phase transitions are of the first order nature [16,19,20]. For the samples with $x = 0.13, 0.3$ and 0.4 , the metal–insulator transition temperatures, defined by the temperatures of resistivity maxima in warming (cooling) runs, were 241 K (239 K), 164 K (162 K) and 156 K (152 K), respectively. In general, the transition temperature in warming process is slightly higher than that in cooling process, especially for those samples having larger x values [16].

Before photoelectron spectroscopy study, all samples were annealed again in oxygen at 900°C for 18 h to ensure the correct amount of oxygen content. These samples were attached to OFHC (oxygen-free high-conducting) copper by good-conducting silver epoxy. UPS measurements were performed both at liquid nitrogen temperature (90 K) and room temperature (295 K) using the high-resolution photoemission chamber equipped with a hemispherical electron energy analyzer manufactured by VG Scientific Inc. The base pressure in the chamber was in the low 10^{-10} or high 10^{-11} Torr range. At room temperature, all spectra show charging effects. So binding energies were calibrated using the Fermi edge (E_F) of a clean Au plate sample. The instrumental resolution was ~ 50 meV with He I photon source ($h\nu = 21.2$ eV). In order to obtain fresh, clean surfaces, the samples were scraped in situ with a diamond file at each measurement and the scraping was made until the contamination-related feature around 9–10 eV binding energy disappeared, so that the whole spectrum did not change with further scraping. Special attention was also paid to the intensity of the feature around 6 eV, which increases with surface degradation. The degradation was so fast that we had less than 15 min to finish the whole scanning.

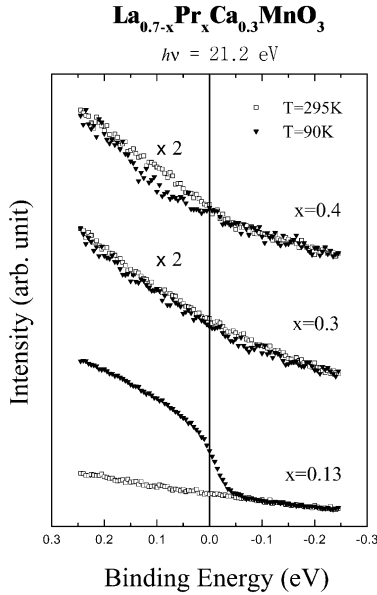


Fig. 1. UPS spectra near the Fermi level for $\text{La}_{0.7-x}\text{Pr}_x\text{Ca}_{0.3}\text{MnO}_3$ samples with $x = 0.13, 0.3$ and 0.4 at room temperature and 90 K using He I photon source ($h\nu = 21.2\text{ eV}$). For $x = 0.13$ sample, the sharp metallic edge at the Fermi level is clearly seen at 90 K .

To confirm the metal–insulator transition, we first looked at the spectral density near the Fermi level with high resolution photoelectron spectroscopy. Fig. 1 shows the temperature dependence of spectral weight near E_F for $x = 0.13, 0.3$ and 0.4 . Clearly, we can see the great enhancement of spectral weight near E_F in the $x = 0.13$ sample when temperature is lowered from room temperature to 90 K . The clear metallic Fermi edge indicates that the sample undergoes a transition from an antiferromagnetic insulator to a ferromagnetic metal as the temperature is below T_c . However, for $x = 0.3$ and 0.4 , the spectra show negligible changes as temperature decreases, and no metallic Fermi edges can be found at 90 K . This is unusual because 90 K is lower than any T_c of the three samples. A similar behavior has also been seen in several manganite systems [10–14, 21–23], where no significant changes with decreasing temperature in the spectral density near E_F and no metallic Fermi edges were found even in the ferrometallic phase. This behavior has been suggested to be due to pseudo-gap phenomena [21–23]. In the present case of LPCMO samples, the optical conductivity data also showed drastic decrease of effective carrier density N_{eff} with increasing Pr content as mentioned above [19,20]. Hence our high resolution photoelectron spectroscopy data may indicate that the reduced ferromagnetic ordering and the greatly enhanced lattice distortion at high Pr doping level indeed give rise to the disappearance of metallic Fermi edge in the $x = 0.3$ and 0.4 samples at 90 K . However, the possibility of the surface effect, where the transport property of the surface probed by the photoelectron spectroscopy is

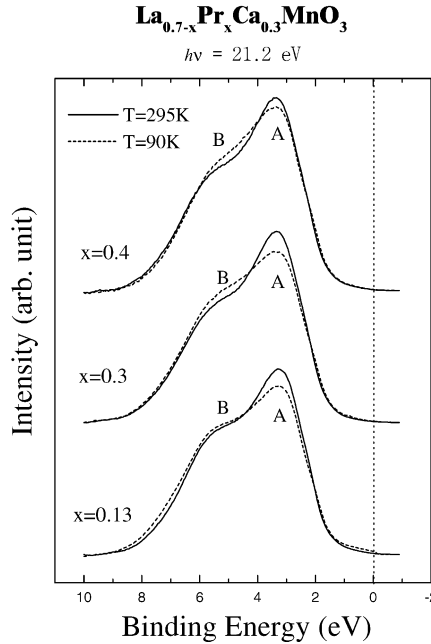


Fig. 2. UPS spectra for the wide valence band region for $\text{La}_{0.7-x}\text{Pr}_x\text{Ca}_{0.3}\text{MnO}_3$ samples with $x = 0.13, 0.3$ and 0.4 at room temperature and 90 K . Strong temperature dependence of spectral weights are shown for all samples.

different from that of the bulk, or the pseudo-gap phenomena cannot be discarded either.

Fig. 2 shows the valence region spectra at room temperature and 90 K for various x values. These spectra were obtained by performing traditional integral background subtraction and peak area normalization on the original spectra. We note that other background correction methods and normalization processes such as linear background subtraction, non-subtraction and dividing by noise weight above E_F due to the higher order photons produce slightly different final spectra, but the major trends remain the same. In Fig. 2, we see the strong temperature dependence of spectral weights, i.e. when we go down from room temperature to 90 K , the relative intensity of the peak A decreases while that of the peak B increases for all samples. This unusual temperature dependence of spectra over the whole VB region was also found in $\text{La}_{1-x}\text{Sr}_x\text{MnO}_3$ [11–13] and is considered to be a unique feature for CMR materials, because no similar temperature dependence was observed in another DE system $\text{La}_{1-x}\text{Sr}_x\text{CoO}_3$ [13].

In Fig. 3, we also show the doping dependence of VB spectra at (a) room temperature and (b) 90 K . It is evident that there is also a spectral weight transfer from peak B to peak A at room temperature when Pr content x increases from 0.13 to 0.3 , although as x continues to increase up to 0.4 negligible spectral change can be found. We can also see the spectral weight transfer from peak B to peak A when x increases from 0.13 to $0.3(0.4)$ at 90 K (Fig. 3b), although the band width is slightly narrowed at the same time in this

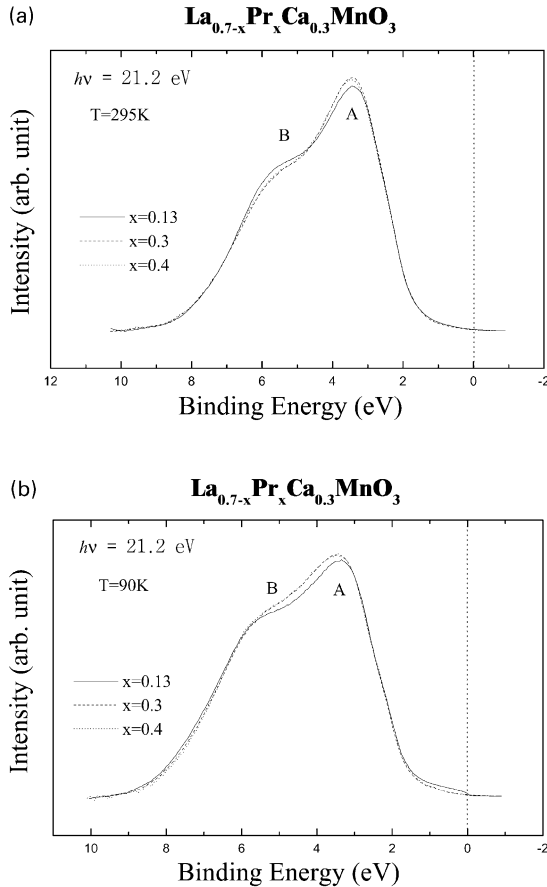


Fig. 3. Doping dependence of UPS spectra in the whole valence band region at (a) room temperature and (b) 90 K.

case. Note that the Pr doping does not introduce any hole into the system, so this doping dependence of spectral weight is very different from that observed in $\text{La}_{1-x}\text{Sr}_x\text{MnO}_3$ [13], where the Sr doping increases the hole density.

To understand the temperature dependence and doping dependence of spectral weight shown in Figs. 2 and 3, we must at first assign the features in valence band correctly. Up to now, many theoretical and experimental studies have been performed on the electronic structures of manganite systems, but the assignments of various spectral features in the valence band are still controversial. The band structure calculation using the local spin density approximation (LSDA) [11,12] predicts that the Mn 3d bands are located near E_F and the O 2p level is below Mn 3d at the binding energy of ~ 5 eV. On the other hand, the LDA + U calculation [24] claims that the inclusion of the electron correlation energy between Mn 3d electrons reverses this order, with O 2p band near the Fermi level while Mn 3d states are located far below. The configuration-interaction cluster model calculation including electron correlations [25] also predicts that the manganites are charge-transfer insulators with the $d^{\underline{n}}L$ (underline denotes a hole) states at

the top of the valence band. Experimentally, the Mn 3d states are usually obscured in UPS owing to the dominant O 2p cross section at low photon energies [26]. Moreover, the strong hybridization between O 2p and Mn 3d states in manganites makes spectral features of heavily mixed character, and it is difficult to extract Mn 3d bands from VB spectra. Hence some experiments utilizing the Mn 2p–3d resonance [10], spin-resolved photoemission [27] and other approaches [11,12,14,15] identified Mn t_{2g} and e_g states at ~ 2.2 and 1.2 eV from E_F in agreement with LDA calculation [11,12], while others [13] followed the assignments of the cluster model calculation. We note that in many 3d transition metal compounds including manganites electron correlation effects are well known to be quite important. In fact, in a systematic study of 3d transition metal compounds, the on-site d–d Coulomb interaction U for manganese oxides is found to be 7–8 eV [28]. This strong on-site Coulomb interaction can drastically change the distribution of spectral weight, as shown in the LDA + U calculation or configuration-interaction cluster model calculation. Hence careful assessments of photoemission peaks are necessary to make correct assignments of their origin.

In our experiment, we used the photon energy $h\nu = 21.2$ eV, and the ratio between Mn 3d and O 2p photoionization cross sections is only $\sim 3\%$ [25,26]. So all the spectral weight and its change may be considered to reflect primarily the O 2p character. Previous experiments found that at higher photon energies where the relative cross section of Mn 3d to O 2p levels becomes stronger, the features near ~ 6 and ~ 2 eV are enhanced relative to the feature at ~ 3 eV [13,15]. This implies that the feature at ~ 3 eV (peak A) has a dominant O 2p character, whereas the ~ 6 eV feature (peak B) has a mixed character, consisting of both O 2p and Mn 3d states. Thus, we can assign peak A to the primarily O 2p non-bonding states and peak B to the O 2p–Mn 3d bonding states, in agreement with *T. Saitoh et al.* [13]. With this assignment, we can explain naturally the temperature and doping dependence of the spectra weights observed in Figs. 2 and 3 as follows—as the mixing between Mn 3d and O 2p levels becomes stronger by the change of temperature (low temperature) or Pr doping level (smaller x value), the weight of peak B relative to that of peak A becomes enhanced. (The negligible difference of spectral weight between $x = 0.3$ and 0.4 may be due to the negligible change of p–d hybridization strength when Pr content increases from 0.3 to 0.4. The closeness of T_c and effective carrier density of the two samples supports this view.). Since the intensity of peak A, which comes from primarily non-bonding states, should remain the same in the zeroth order approximation, this change of spectral weight mostly reflects the degree of mixing of O 2p states in the bonding level peak B. The fact that O 2p contribution becomes larger in this bonding level when the hybridization becomes stronger implies that the binding energy of ‘bare’ O 2p level should be lower than that of Mn 3d level before the

hybridization is turned on. This ordering of Mn 3d and O 2p levels is opposite to the energy level diagram of the LSDA calculation [11,12], but consistent with those of the LDA + U or configuration-interaction cluster model calculations. Hence, we can conclude that our photoemission data on LPCMO support the importance of electron correlation effect in these compounds, and suggest that the discussion on their electronic structures should be based on the energy level scheme of LDA + U or cluster-model calculations rather than the commonly used LSDA calculation.

In summary, we have studied the UPS of LPCMO and found unusual temperature and doping dependences of spectral weights in the whole valence band region. These spectral weight transfers are mainly due to the change of the Mn 3d–O 2p hybridization strength with temperature and Pr doping, and can be understood by the energy level diagram of LDA + U or cluster-model calculations, but are not consistent with LSDA calculation. This shows the importance of electron correlation effect in the electronic structures of these manganites. The experimental spectral density near the Fermi level also depends on the temperature and Pr doping, which may be due to the ferromagnetic order and lattice distortion effects as well as pseudo-gap phenomena or surface effect.

Acknowledgments

The authors would like to thank Profs Tae Won Noh at Seoul National University for preparing samples and informative discussions. This work is supported in part by the Korean Science and Engineering Foundation through Center for Strongly Correlated Materials Research and

Grant No. 976-0200-005-2, and by the Ministry of Education through BSRI-97-7401.

References

- [1] S. Jin, et al., *Science* 264 (1994) 413.
- [2] C. Zener, *Phys. Rev.* 82 (1951) 403.
- [3] P.W. Anderson, H. Hasegawa, *Phys. Rev.* 100 (1955) 675.
- [4] P.G. de Gennes, *Phys. Rev.* 118 (1960) 141.
- [5] A.J. Millis, P.B. Littlewood, B.I. Shraiman, *Phys. Rev. Lett.* 77 (1996) 175.
- [6] A.J. Millis, *Phys. Rev. B* 54 (1996) 5389.
- [7] A.J. Millis, *Nature* 392 (1998) 147.
- [8] C.H. Booth, et al., *Phys. Rev. Lett.* 80 (1998) 853.
- [9] D. Louca, et al., *Phys. Rev. B* 56 (1997) 8475.
- [10] J.-H. Park, et al., *Phys. Rev. Lett.* 76 (1996) 4215.
- [11] D.D. Sarma, et al., *Phys. Rev. Lett.* 75 (1995) 1126.
- [12] D.D. Sarma, et al., *Phys. Rev. B* 53 (1996) 6873.
- [13] T. Saitoh, et al., *Phys. Rev. B* 56 (1997) 8836.
- [14] A. Chainani, et al., *Phys. Rev. B* 56 (1997) R15513.
- [15] J.-S. Kang, et al., *Phys. Rev. B* 60 (1999) 13257.
- [16] H.Y. Hwang, et al., *Phys. Rev. Lett.* 75 (1995) 914.
- [17] K.H. Kim, et al., *Phys. Rev. B* 55 (1997) 4023.
- [18] K.H. Kim, et al., *Phys. Rev. Lett.* 81 (1998) 4983.
- [19] K.H. Kim, PhD Thesis, Seoul National University.
- [20] D.J. Eom, MS Thesis, Seoul National University.
- [21] D.S. Dessau, et al., *Phys. Rev. Lett.* 81 (1998) 192.
- [22] T. Saitoh, et al., *Phys. Rev. B* 62 (2000) 1039.
- [23] Y.-D. Chuang, et al., *Science* 292 (2001) 1509.
- [24] S. Satpathy, Z.S. Popovic, F.R. Vukajlovic, *Phys. Rev. Lett.* 76 (1996) 960.
- [25] T. Saitoh, et al., *Phys. Rev. B* 51 (1995) 13942.
- [26] J.J. Yeh, I. Lindau, *At. Data Nucl. Data Tables* 32 (1985) 1.
- [27] J.-H. Park, et al., *Nature* 392 (1998) 794.
- [28] A.E. Bocquet, et al., *Phys. Rev. B* 46 (1992) 3771.